



1  
2  
3  
4  
5  
6  
7  
8  
9  
10 **Dr. M.T, Mangan**  
11 **Journal of Volcanology and Geothermal Research**  
12 **Editor in Chief**

13  
14 Reykjavík, dags,  
15

16 Dear editor

17 Enclosed is the manuscript: *Gas emissions and crustal deformation from the Krýsuvík high*  
18 *temperature geothermal system, Iceland*. Authors are: myself, Evgenia Ilynskaya, Sigrún  
19 Hreinsdóttir, Baldur Bergsson, Karolina Michakczewska, Alessandro Aiuppa and Auður Agla  
20 Óladóttir. We would like to submit the manuscript as an article for Journal of Volcanology and  
21 Geothermal Research. The manuscript consists of a main text, 9 color figures (requested black and  
22 white in print verison) and 5 tables.

23  
24 I am the corresponding author for this article and may be contacted (see details below)  
25 regarding the revision process. I confirm that this work has not been published, nor is  
26 under consideration for publication elsewhere.

27  
28 This article focuses on gas emissions and crustal deformation in Krýsuvík high-  
29 temperature geothermal system. Based on that, we suggest that the following individuals  
30 are highly qualified to act as Reviewers for this manuscript:

- 31 1. Giovanni Chiodini, INGV Bologna, giovanno.chiodini@ingv.it
- 32 2. P. A. Hernández, Instituto Volcanológico de Canarias (INVOLCAN), Spain,  
33 phdez@iter.es
- 34 3. Tasmin Mather, University of Oxford, tasmin.mather@earth.ox.ac.uk
- 35 4. Luigi Marini, Via Antonio Fratti, 253 I-55043, Viareggio, Italy,  
36 luigomarini@rocketmail.com
- 37 5. Clive Oppenheimer, Department of Geography, University of Cambridge, Downing  
38 Place, Cambridge CB2 3EN, UK, clive.oppenheimer@geog.cam.ac.uk
- 39 6. Rossella Di Napoli, University of Palermo, Italy, rossella.dinapoli@unipa.it

40  
41 Sýlvía Rakel Gudjónsdóttir, Sjávargata 11, 225 Gardabaer, Iceland.– Tel. +3548478611 —  
42 e-mail: srg@isor.is

# Gas emissions and crustal deformation from the Krýsuvík high temperature geothermal system, Iceland.

Sylvía Rakeł Gudjónsdóttir (1), Evgenia Ilyinskaya (2), Sigrún Hreinsdóttir (3), Baldur Bergsson (4), Karolina Michakczewska (5), Alessandro Aiuppa (6), Audur Agla Óladóttir (1)

(1) Iceland GeoSurvey, Grensásvegur 9, 108 Reykjavík, Iceland

(2) School of Earth and Environment, University of Leeds, Leeds, LS7 4LR, United Kingdom

(3) GNS Science, PO Box 30368, Lower Hutt 5040, New Zealand

(4) Icelandic MetOffice, Bústaðarvegi 7-9, 108 Reykjavík, Iceland

(5) Institute of Earth Sciences, University of Iceland, Sturlugata 7, Askja, 101 Reykjavík, Iceland

(6) Università di Palermo DiSTeM, Palermo, Italy

## Abstract

The Krýsuvík volcanic system is located at the oblique spreading Reykjanes Peninsula, SW Iceland. Since early 2009 the region has been undergoing episodes of localized ground uplift and subsidence. In April 2013, near-real time monitoring of gas emissions was started in Krýsuvík using a Multi-component Gas Analyzer System (Multi-GAS), collecting data on gas composition ( $\text{H}_2\text{O}$ ,  $\text{CO}_2$ ,  $\text{SO}_2$ ,  $\text{H}_2\text{S}$ ). Gas emissions from Krýsuvík geothermal system are examined and correlated with crustal deformation and seismicity. The dataset comprises near-continuous gas composition time series (Multi-GAS), quantification of diffuse  $\text{CO}_2$  gas flux, direct samples of dry gas, seismic records, and GPS data.

The gas emissions from the Krýsuvík system are  $\text{H}_2\text{O}$ -dominated, with  $\text{CO}_2$  as the most abundant dry gas species, followed by lesser amounts of  $\text{H}_2\text{S}$ . The average subsurface equilibrium temperature was calculated as  $278^\circ\text{C}$ . This is consistent with previous observations made through sporadic spot sampling campaigns. In addition, the semi-continuous Multi-GAS dataset reveals higher variations of gas composition than previously reported by spot sampling.

The diffuse soil  $\text{CO}_2$  flux is found to be variable between the three degassing areas in Krýsuvík ranging from 10.9-70.9 T/day, with the highest flux in Hveradalir where the Multi-GAS station is located. The total flux is estimated as 101 T/day.

Comparison between Multi-GAS and geophysical data shows that peaks of  $\text{H}_2\text{O}$ -rich emissions follow events of crustal movements. Coinciding with the  $\text{H}_2\text{O}$ -rich peaks,  $\text{SO}_2$  is detected in minor amounts ( $\sim 0.6$  ppmv), allowing for calculations of  $\text{H}_2\text{O}/\text{SO}_2$ ,  $\text{CO}_2/\text{SO}_2$  and  $\text{H}_2\text{S}/\text{SO}_2$  ratios. This is the first time  $\text{SO}_2$  has been detected in the Krýsuvík area.

The large variations in  $\text{H}_2\text{O}/\text{CO}_2$  and  $\text{H}_2\text{O}/\text{H}_2\text{S}$  ratios are considered to reflect variable degassing activity in the fumarole. The activity of the fumarole appears less intense during intervals of low or no recorded seismic events. The  $\text{H}_2\text{O}/\text{CO}_2$  and  $\text{H}_2\text{O}/\text{H}_2\text{S}$  ratios are lower, presumably due to  $\text{H}_2\text{O}$  condensation processes affecting the steam jet before reaching the Multi-GAS inlet tube.

**Keywords:** Krýsuvík, volcanic gas, volcano monitoring, geothermal gas, crustal deformation, volcanic  $\text{CO}_2$  flux

# 87 1 Introduction

88 Monitoring volcanic and geothermal gases, along with seismicity and ground deformation,  
89 can lead to better understanding of volcano behaviour, and can provide early warning of  
90 volcanic activity. Several studies have focused on quiescent degassing from active volcanic  
91 and geothermal systems, detecting peaks of increased gas emissions prior to eruptions  
92 (e.g., Young et al., 1998, Aiuppa et al., 2010). It has been shown that, under certain  
93 conditions, seismicity and ground deformation may help releasing gases into geothermal  
94 systems and increase fumarolic emission (e.g., Watson et al., 2000, Italiano et al., 1998,  
95 Toutain and Baubron, 1999, Chiodini et al., 2012, 2015, and references therein).  
96 Monitoring of soil CO<sub>2</sub> diffuse degassing in geothermal areas has also proven to give  
97 reliable information on the mass/energy budget of utilized and non-utilized geothermal  
98 systems (Brombach et al., 2001; Chiodini et al., 2001, Fridrikson, 2006, Óladóttir, 2012).  
99 In Iceland, there has been limited research on the relationship between degassing from high  
100 temperature geothermal areas (where temperature at 1 km depth is greater than 200°C) and  
101 seismic energy release and ground deformation (Ref?). The Krýsuvík volcanic system,  
102 located on the oblique spreading Reykjanes Peninsula (RP), is characterized by abundant  
103 degassing through soil and fumaroles within a high-temperature geothermal area. It has  
104 high seismic activity, characterized by swarms of micro-earthquakes as well as main-  
105 shock/aftershock sequences (Klein et al., 1977 and references therein, Ward and  
106 Björnsson, 1971, Kristjánsdóttir, 2013). In the last decade the region has undergone  
107 episodes of uplift and subsidence, with high seismic activity occurring during periods of  
108 uplift (Michalczewska et al., 2012).  
109 Here we present semi-continuous, near-real time gas measurements in the Krýsuvík  
110 geothermal system. Such measurements are relatively new in Iceland with the first station  
111 installed on top of Mt. Hekla volcano in 2012 (Ilyinskaya et al., 2015; Di Napoli et al.,  
112 2016). In this study we evaluate the gas composition emitted from the Krýsuvík  
113 geothermal system and interpret its origin. This is done through analysis of a semi-  
114 continuous time series of gas composition (Multi-GAS sensor system, e.g., Aiuppa 2009),  
115 direct steam sampling of fumaroles, and quantification of the diffuse CO<sub>2</sub> flux from the  
116 geothermally active areas (accumulation chamber method, e.g., Fridriksson et al., 2006).  
117 We correlate the gas time series with geophysical observations from Krýsuvík (ground  
118 deformation and seismicity).

## 119 1.1 Regional settings

120 Krýsuvík is one of five active, NE-SW trending, volcanic systems located on the RP  
121 (Saemundsson et al., 2010, Hreinsdóttir et al., 2001, Einarsson, 2008) (Figure 1). The  
122 system is thought to be in an early stage of evolution, dominated by rift volcanism with no  
123 major magma chamber (Arnórsson et al., 1975). Volcanic activity is periodic with roughly  
124 1000 years intervals between eruptive episodes, each eruptive episode lasting for 400-500  
125 years (Saemundsson et al., 2006, Jónsson, 1978). The last volcanic eruption in Krýsuvík  
126 took place in the 12<sup>th</sup> century (Saemundsson and Sigurgeirsson, 2013). Krýsuvík currently  
127 hosts a high-temperature geothermal system, the heat source of which is considered to be  
128 dyke intrusions (Arnórsson et al., 1975, Arnórsson, 1987). Recent resistivity measurements  
129 within the Krýsuvík system indicate a conductive body at approximately 2 to 5 km depth  
130 (Didana, 2010, Hersir et al., 2013). This body is located near the central part of the  
131 Krýsuvík geothermal area, with an approximate size of 10 km<sup>2</sup>, and coincides with the  
132 source of the inflation and deflation observed with GPS and InSAR measurements

133 (Michalewska et al., 2012, Hersir et al., 2013). The lack of S-wave attenuation in the  
134 region has been used as an argument against the presence of large volumes of molten  
135 materials, but rather the presence of a gaseous or supercritical fluid (Adelinet et al., 2011).

136 The Krýsuvík geothermal system is often split into 6 subareas: Sandfell, Trölladyngja,  
137 Köldunámur, Seltún, Hveradalir, and Austurengjar (Figure 2). This study is focused on the  
138 last three, which have the highest and most continuous geothermal surface activity  
139 including hot and altered ground with mud pools, fumaroles, and local solfataras. The main  
140 surface activity is confined to the Vesturháls and Sveifluháls hyaloclatite ridges (including  
141 Seltún and Hveradalir), and a fault through a boiling dilute mud pool in Austurengjar  
142 (Austurengjahver) east of the Sveifluháls ridge (Markússon and Stefánsson, 2011).  
143 Resistivity measurements indicate that the geothermal subareas within Krýsuvík, originate  
144 from one and the same system of an approximate size of 40-60 km<sup>2</sup> (Gudmundsson et al.,  
145 1975, Saemundsson and Sigurgeirsson, 2013) (Figure 2).

## 146 **2 Methodology and data processing**

### 147 **2.1 Gas composition analysis using MultiGAS and direct** 148 **fumarole sampling**

149 A Multi-component Gas Analyzer System station (Multi-GAS, INGV-type, see e.g.,  
150 Aiuppa 2009, Ilyinskaya et al., 2014) was installed on 26 April 2013 at Hveradalir in  
151 Krýsuvík (Figure 3), next to a fumarole in an area of high and persistent surface  
152 geothermal activity. Data collection was discontinued over a short period from 27 June – 5  
153 July 2013 when the station was needed for another project. The sampling intake was ~20  
154 cm above ground level (Figure 3), which was necessary to avoid saturation of the  
155 CO<sub>2</sub> sensor. The station was powered by a permanent wind turbine and was configured to  
156 acquire data in cycles of 200 samples, each being the median of 9 measurements @ 1 Hz  
157 (30 minutes per sampling cycle). A time interval of 6 hours between sampling cycles was  
158 set. A 3G radio modem was used for telemetry, and data were retrieved remotely using  
159 custom-made software (Ratiocalc 2.0, Tamburello, 2015) which allows for automatic  
160 creation of gas species scatter plot from the acquired data. The gas molar ratios were  
161 calculated from the gradient of best fit regression lines (Aiuppa et al., 2009, 2010) and  
162 calculations were restricted to intervals when measured concentrations showed substantial  
163 excess relative to ambient air (see e.g., Ilyinskaya, 2014). Overall uncertainty in the  
164 derived ratios is ≤20% (Aiuppa et al., 2009).  
165

166 A total of 8 samples of dry gas were collected in two campaigns with 8-week interval (four  
167 samples each time, Figure 2) from fumaroles with a focussed steam flow (four samples in  
168 Hveradalir, two in Seltún, and two in Austurengjar). The samples were collected into  
169 evacuated double port bottle with 25 ml of a 10M NaOH solution. The ground temperature  
170 next to the fumarole was recorded and was in all cases >97°C.

171 The dry gas samples were analysed for gas composition using standard procedures at the  
172 Iceland GeoSurvey (ÍSOR), Reykjavík, Iceland. Headspace gases (N<sub>2</sub>, CH<sub>4</sub>, Ar, H<sub>2</sub>, and

173 O<sub>2</sub>) were analysed for using gas chromatography in a Perkin-Elmer Arnel 4019 gas  
174 chromatograph. CO<sub>2</sub> and H<sub>2</sub>S were analysed for by titration of the caustic solution.

## 175 **2.2 Soil temperature and diffuse CO<sub>2</sub> flux through soil**

176 The soil CO<sub>2</sub> flux was measured using a West Systems fluxmeter in the three studied sub-  
177 areas of Krýsuvík using the accumulation chamber method (e.g., Fridriksson et al., 2006).  
178 The method has proven to be an accurate way to measure soil CO<sub>2</sub> fluxes in volcanic and  
179 geothermal areas, where it does not require assumptions or corrections that depend on soil  
180 characteristics (Chiodini et al., 1998). The measurements were carried out on  
181 approximately 25×25 meter grid, where possible. The total number of measurement points  
182 was 435; 217 of which were in Hveradalir, 136 were in Seltún, and the remaining 82 were  
183 in Austurengjar. Most of the measurements were taken in late summer or autumn, during  
184 dry and calm weather conditions to avoid the influence of external weather factors and  
185 water saturation of the soil. The average time of each measurement was 1-2 minutes,  
186 depending on the time the rate of CO<sub>2</sub> concentration increase stabilized. To evaluate the  
187 total CO<sub>2</sub> emission from the measured areas the Kriging algorithm (Cardellini et al., 2003,  
188 and references therein) was used for interpolation. The soil temperature was measured with  
189 a handheld digital thermometer with a 15 cm long probe.

## 190 **2.3 Geophysical data**

191 Seismic and GPS data from Krýsuvík were used to correlate with the gas measurements.  
192 The seismic data were provided by the Icelandic Meteorological Office (IMO) from the  
193 SIL seismic network.

### 194 **2.3.1 Seismic data**

195 The seismic data included 217 events in the Krýsuvík region occurring from late April  
196 through November 2013. The seismic moment was used to estimate the moment  
197 magnitude,  $M_w$  (Hanks and Kanamori, 1979):

$$198 \quad M_w = \frac{2}{3(\log_{10}[(M_0) - 9.1])} \quad (1)$$

199 The largest recorded seismic event for the study period was  $M_w$  2.2 on 11 July 2013. The  
200 frequency-magnitude distribution (Gutenberg and Richter, 1944) for the Krýsuvík  
201 catalogue gives a magnitude of completeness,  $M_w$  0.75 and the slope or b-value of 1.6. All  
202 events  $M_w < 0.75$  were discarded from further analysis, leaving a total of 172 events.

203 The global average b-value is around 1 but ranges locally from 0.5-2 depending on factors  
204 like the type of tectonic environment and stress. Keiding et al., (2009) used data spanning  
205 1997 to 2006 to evaluate the b-value for the Krýsuvík region, giving a considerably lower  
206 value of 0.9. The dataset used here (172 events) is considerably smaller which could bias  
207 the estimate. However, high b-values are often observed in volcanic and geothermal  
208 regions and assumed to be related to heterogeneous crust as well as local stress  
209 perturbations and fluids (Wyss, 1973, Schorlemmer et al., 2005).

210 The daily cumulative seismic moment was estimated showing several peaks of increased  
211 seismic activity over the study period, with the largest one occurring in mid-July.

## 212 2.3.2 GPS data

213 The GPS station MOHA started continuous operation in 2010 to monitor crustal  
214 deformation in the Krýsuvík region. The station is located just north of the center of uplift  
215 observed from 2010 to 2011 (Figure 1).

216 GPS data were analysed using GAMIT/GLOBK version 10.4 using over 100 continuous  
217 global GPS stations to evaluate average daily site positions in the ITRF08 reference frame.  
218 In the processing we solve for station coordinates, satellite orbit and earth rotation  
219 parameters, atmospheric zenith delay every two hours, and three atmospheric gradients per  
220 day. The IGS08 azimuth and elevation dependent absolute phase center offsets were  
221 applied to all antennas and ocean loading was corrected for using the FES2004 model. To  
222 minimize common mode signal in the time series the de-trended time series from the GPS  
223 station NYLA, outside the deforming region, were subtracted from the data. The running  
224 weighted average of seven days for the dataset was then calculated. The calculated total  
225 subsidence during the year of 2013 was  $\approx 21$  mm. Figure 4 shows clearly the local  
226 inflation/deflation periods in the last decade from the GPS time series (2007-2016) of  
227 vertical crustal movements at station MOHA, just north of the inflation center (Figure 1),  
228 along with daily cumulative seismic moment for the region.

## 229 3 Results

### 230 3.1 Assessment of the influence of meteorological conditions 231 on the MultiGAS data

232 Before interpreting the MultiGAS data, we assessed the influence of meteorological  
233 conditions on the measurements. The gas ratios ( $\text{H}_2\text{O}/\text{CO}_2$ ,  $\text{H}_2\text{O}/\text{H}_2\text{S}$ ,  $\text{H}_2\text{O}/\text{SO}_2$ ,  $\text{CO}_2/\text{H}_2\text{S}$ ,  
234  $\text{CO}_2/\text{SO}_2$ ,  $\text{H}_2\text{S}/\text{SO}_2$ ) were compared against wind speed (m/s) and precipitation (mm/day)  
235 data. Wind data from the three weather stations closest to the location of the MultiGAS  
236 station were investigated: Festarfjall, Selvogur and Straumsvík (IMO monitoring data).  
237 Based on the topography of the area it was considered that the atmospheric conditions are  
238 the most similar between the locations of the Festarfjall weather station and the MultiGAS  
239 station (Figure 1). The wind dataset from the Festarfjall station consists of hourly  
240 measurements. This resolution allows for an accurate comparison between the wind speed  
241 and each MultiGAS acquisition. MultiGAS data were acquired for 30 min starting at  
242 00:00, 06:00, 12:00 and 18:00 each day. The precipitation data (IMO monitoring data) was  
243 obtained from the Keflavík airport station (Figure 1), collected twice per day (09:00 and  
244 18:00). The representative precipitation is taken to be the total precipitation per day (where  
245 one day is defined from 18:00-18:00 UTC), and used to compare with all MultiGAS  
246 acquisitions made that same day.

247 All gas molar ratios were predominately observed and showed the highest fluctuations  
248 during dry periods ( $< 2$  mm/day). However, high values for  $\text{CO}_2/\text{H}_2\text{S}$ ,  $\text{CO}_2/\text{SO}_2$  and  
249  $\text{H}_2\text{S}/\text{SO}_2$  ratios are not confined to the dry periods since these gas species are less affected  
250 by condensation during rainy days than  $\text{H}_2\text{O}$ . Figure 5 shows the  $\text{CO}_2/\text{H}_2\text{S}$  and  $\text{H}_2\text{O}/\text{CO}_2$   
251 gas ratios compared with precipitation (mm/day).

252 During periods of low wind speed (<5 m/s) the CO<sub>2</sub>/H<sub>2</sub>S, CO<sub>2</sub>/SO<sub>2</sub> and H<sub>2</sub>S/SO<sub>2</sub> ratios  
253 show the highest fluctuation. Progressive decrease in obtained CO<sub>2</sub>/H<sub>2</sub>S, CO<sub>2</sub>/SO<sub>2</sub> and  
254 H<sub>2</sub>S/SO<sub>2</sub> ratios and decrease in fluctuation of the ratios is observed with higher wind  
255 speeds. No visual correlation is apparent between the H<sub>2</sub>O/X ratios (where X stands for  
256 CO<sub>2</sub>, H<sub>2</sub>S and SO<sub>2</sub>) with wind speed below 10 m/s. Markedly fewer ratios are obtained  
257 when wind speed exceeds 10 m/s. Figure 5 shows the H<sub>2</sub>O/CO<sub>2</sub> and CO<sub>2</sub>/H<sub>2</sub>S gas ratios  
258 compared with wind speed (m/s).

259 Based on these results it was decided to eliminate all gas molar ratios obtained during days  
260 of more than 2 mm/day of precipitation. Additionally, CO<sub>2</sub>/H<sub>2</sub>S, CO<sub>2</sub>/SO<sub>2</sub> and H<sub>2</sub>S/SO<sub>2</sub>  
261 ratios collected in periods of wind speed above 5 m/s were eliminated. This allows for  
262 using only ratios calculated from concentrations deemed slightly or not affected by the  
263 meteorological conditions, for correlation with geophysical observations.

### 264 **3.2 Gas composition**

265 The fumarole gas samples from Krýsuvík were dominated by H<sub>2</sub>O (96.6-99.6 vol%) with  
266 CO<sub>2</sub> as the dominant dry gas component (on average 83.8 vol%), followed by much  
267 smaller amounts of H<sub>2</sub>S (on average 9.17 vol%), hydrogen (H<sub>2</sub>), nitrogen (N<sub>2</sub>), methane  
268 (CH<sub>4</sub>) and argon (Ar) (Table 1). One sample (Seltún 1) had a small component of O<sub>2</sub>, a  
269 result of atmospheric contamination during sampling.

270 The detected MultiGAS ratios (where effects of the meteorological conditions have been  
271 eliminated) are shown to be highly variable (Table 2). Minor amounts of SO<sub>2</sub> were  
272 measured for the first time in Krýsuvík by the MultiGAS sensor. The measured SO<sub>2</sub>  
273 concentrations are very low but the bulk (63%) is above the detection limit (0.05 ppmv) of  
274 the MultiGAS sensor, allowing for calculations of the X/SO<sub>2</sub> ratios (X = H<sub>2</sub>O, CO<sub>2</sub> and  
275 H<sub>2</sub>S). Concentrations below 0.05 ppmv are considered to be instrumental noise. The SO<sub>2</sub>  
276 sensor is not quantitative below 1 ppmv so the measurements (0.05-1 ppmv) should only  
277 be viewed as qualitative assessments of SO<sub>2</sub> presence with a great uncertainty.

278 The calculated ratios of H<sub>2</sub>O/CO<sub>2</sub>, H<sub>2</sub>O/H<sub>2</sub>S and CO<sub>2</sub>/H<sub>2</sub>S from the fumarole samples are  
279 compared to the MultiGAS ratios in Table 3. The average value for H<sub>2</sub>O/CO<sub>2</sub> and H<sub>2</sub>O/H<sub>2</sub>S  
280 from the fumarole samples (220 and 2812, respectively, excluding Seltún 1 sample), fall  
281 within the range of the highest H<sub>2</sub>O/CO<sub>2</sub> and H<sub>2</sub>O/H<sub>2</sub>S ratios measured by the MultiGAS  
282 sensor (220 and 10,000, respectively). For CO<sub>2</sub>/H<sub>2</sub>S, the average and median values of the  
283 fumarole samples (13 and 10, respectively) are close to the average and the median values  
284 of the MultiGAS data (17 and 12, respectively).







### 285 **3.3 Soil CO<sub>2</sub> flux and temperature**

286 The highest soil CO<sub>2</sub> diffuse degassing was found in areas with intense surface activity, where steam rises through fissures and cracks towards  
287 the surface, mostly in the three observation sites (total 0.31 km<sup>2</sup>). The CO<sub>2</sub> fluxes ranged between 0 and 29,200 g m<sup>-2</sup> day<sup>-1</sup> with an average  
288 value of 385 g m<sup>-2</sup> day<sup>-1</sup> and median value of 6 g m<sup>-2</sup> day<sup>-1</sup>. In Austurengjar (0.09 km<sup>2</sup>) 80% of all observation points show a very low CO<sub>2</sub>  
289 flux (<10 g m<sup>-2</sup> day<sup>-1</sup>) 68% in Hveradalir (0.140 km<sup>2</sup>) and 51% in Seltún (0.08 km<sup>2</sup>) (Figure 6).

290 The calculation of total flux from the three observation areas shows that the Hveradalir area had by far the greatest total flux of 70.9 T/day.  
291 Next was Seltún with 19.6 T/day and at last Austurengjar with 10.9 T/day. The total CO<sub>2</sub> soil flux from the three observation areas was  
292 estimated as 101 T/day. The soil temperature ranged between 4.2-99.0 °C with the average value 19°C and median value of 12°C.

## 293 **4 Discussion**

### 294 **4.1 Application of gas geothermometers**

295 Gas geothermometers (here: Arnórsson et al., 1998 and Arnórsson and Gunnlaugsson, 1985, Table 4) were used to determine the subsurface  
296 temperature of the Krýsuvík geothermal system based on the fumarole steam composition (Table 5). The gas geothermometers are based on  
297 that the concentrations of CO<sub>2</sub>, H<sub>2</sub>S and H<sub>2</sub> in geothermal reservoir waters are controlled by temperature dependent equilibria with minerals  
298 (Arnórsson and D'Amore, 2000).

299 The lowest individual variations were observed for both the CO<sub>2</sub> geothermometers, indicating sub-surface temperature of 292.6°C (Table 5).  
300 The agreement of other geothermometers was not very good as predicted temperatures varied for individual samples. The average value of the  
301 H<sub>2</sub>S geothermometers was 267°C and of the H<sub>2</sub> 276°C. Also, a substantial discrepancy was observed between the various geothermometers  
302 that is known from previous studies (e.g., Arnórsson et al., 1985).

303 The average sub-surface temperature for all samples was estimated around 278°C which is comparable to previous studies (e.g., Arnórsson  
304 and Gunnlaugsson, 1985, Arnórsson, 1987, Yohannes, 2004).

## 305 **4.2 Correlation of geophysical observations and the MultiGAS data**

306

### 307 **4.2.1 Correlation with H<sub>2</sub>O/CO<sub>2</sub>, H<sub>2</sub>O/H<sub>2</sub>S and X/SO<sub>2</sub> MultiGAS ratios**

308 Distinct periods with peaks in H<sub>2</sub>O/CO<sub>2</sub> and H<sub>2</sub>O/H<sub>2</sub>S gas ratios are observed from the MultiGAS time series. SO<sub>2</sub> was detected almost  
309 exclusively at the same time as these detected peaks, allowing for calculations of X/SO<sub>2</sub> ratios (Figure 7). A visual correlation was observed  
310 between the H<sub>2</sub>O/CO<sub>2</sub> and H<sub>2</sub>O/H<sub>2</sub>S MultiGAS peaks and crustal movements (micro-seismicity and ground deformation detected with  
311 continuous GPS measurements, Figure 7). The largest recorded seismic events for the period of this study were M<sub>w</sub> 2.2 (11 July 2013) and  
312 M<sub>w</sub> 1.5 (26 April 2013). Following these events and throughout the aftershock period (11 July to 7 August and 26 April to 25 May 2013,  
313 respectively) the most extensive increase in the H<sub>2</sub>O/CO<sub>2</sub> and H<sub>2</sub>O/H<sub>2</sub>S MultiGAS ratios were observed. Similarly, moderate increases for the  
314 same gas ratios were observed during periods of moderately sized peaks of accumulative seismic moment. Peaks of high H<sub>2</sub>O/CO<sub>2</sub> and  
315 H<sub>2</sub>O/H<sub>2</sub>S MultiGAS ratios also seemed to follow periods of ground uplift when associated with the recorded seismic events. No gas peaks  
316 were observed during period of subsidence associated with low seismic activity (Figure 7).

317

318 The H<sub>2</sub>O/CO<sub>2</sub> and H<sub>2</sub>O/H<sub>2</sub>S MultiGAS ratios showed greater variations (1-217 and 9-10,300, respectively) than the ratios in our fumarole  
319 samples (H<sub>2</sub>O/CO<sub>2</sub> range 184-269 and H<sub>2</sub>O/H<sub>2</sub>S range 1080-4527). During periods of recorded crustal movements, the H<sub>2</sub>O/CO<sub>2</sub> and H<sub>2</sub>O/H<sub>2</sub>S  
320 MultiGAS ratios increase, and are closer, or equal to the gas ratios in the fumarole samples (Table 3).

321 It is proposed that the high variations in H<sub>2</sub>O/CO<sub>2</sub> and H<sub>2</sub>O/H<sub>2</sub>S MultiGAS ratios are related to the intensity of fumarole activity. The  
322 fumarole activity is low during periods of low or no recorded seismic events and land subsidence (Figure 8). During these periods low  
323 H<sub>2</sub>O/CO<sub>2</sub> and H<sub>2</sub>O/H<sub>2</sub>S MultiGAS ratios are obtained due to significant H<sub>2</sub>O condensation (i.e., removal of H<sub>2</sub>O from the gas phase) before  
324 the steam reaches the inlet tube. Due to the MultiGAS setup in Krýsuvík (inlet 20 cm above ground) the low H<sub>2</sub>O/CO<sub>2</sub> and H<sub>2</sub>O/H<sub>2</sub>S  
325 MultiGAS ratios (<180 and <1000, respectively) are not representative of the emitted fumarole gas composition.

326 The fumaroles are interpreted to be more active during periods of recorded crustal movements. During these periods the steam rises up faster,  
327 because of opening of new pathways and increased boiling by pressure release caused by seismicity (Figure 8). As a result, H<sub>2</sub>O is less  
328 affected by pre-sampling condensation, which results in higher H<sub>2</sub>O/CO<sub>2</sub> and H<sub>2</sub>O/H<sub>2</sub>S gas ratios measured by the MultiGAS.

#### 329 4.2.2 Correlation with CO<sub>2</sub>/H<sub>2</sub>S MultiGAS ratio

330 No visual correlation is observed between CO<sub>2</sub>/H<sub>2</sub>S ratios obtained by the MultiGAS and periods of recorded crustal movements (Figure 9).  
331 These gas species are significantly less affected by condensation processes than H<sub>2</sub>O and their detection was less dependent on the variations  
332 in the activity of the fumarole. The CO<sub>2</sub>/H<sub>2</sub>S ratios obtained from the MultiGAS data generally fall within the range of ratios measured in  
333 fumaroles in Krýsuvík (Figure 9) However, the MultiGAS data show more variability than the fumarole data (this study, Arnórsson, 1987 and  
334 data from the Iceland GeoSurvey database). This is considered to be the result of the MultiGAS station measuring near-continuously for over  
335 7 months, thereby picking out short-timescale variations that may be missed by point sampling. The observed variations in CO<sub>2</sub>/H<sub>2</sub>S ratios are  
336 therefore believed to be linked to variations in the degassing behaviour of the system.

#### 337 4.3 Origin of the Krýsuvík gas emissions

338 The degassing regime in Krýsuvík is shown to be highly variable over short timescales (hours and days) with changes in fumarole activity and  
339 fluctuations in gas composition which is linked to variations in seismicity along with ground deformation. The results from the MultiGAS and  
340 fumarole samples resemble a typical composition of low temperature (<100°C) fumarole steam (Lee et al., 2005) from a liquid dominated  
341 system (Goff and Janik, 2000). The gas composition from this study is in good agreement to previous gas measurements in Krýsuvík (e.g.,  
342 Arnórsson, 1987) and indicates no increased magmatic gas contribution. Therefore we can't conclude that the measured SO<sub>2</sub> is connected with  
343 new magma intruding into the systems' roots.

344 SO<sub>2</sub> concentrations are not expected to be high in geothermal systems like Krýsuvík. This is due to abundant water within the system where  
345 hydrolysis reactions change SO<sub>2</sub> into H<sub>2</sub>S, sulfuric acid (H<sub>2</sub>SO<sub>4</sub>) and elemental sulfur (e.g., Ármannsson et al., 1981, 1989, Ármannsson and  
346 Hauksson, 1980, Gíslason et al., 1978, Óskarsson, 1978, 1984). However, the SO<sub>2</sub> detected here (0.05-0.5 ppmv) is not considered to be a  
347 false signal or interference from other gas species. This is based on two main reasons: (1) SO<sub>2</sub> is observed independently from high  
348 concentrations of H<sub>2</sub>S and therefore the SO<sub>2</sub> measurements are unlikely to be interference between the H<sub>2</sub>S and SO<sub>2</sub> sensors. (2) The  
349 MultiGAS station is equipped with highly sensitive sensors that are capable of detecting very low concentrations. It is considered possible that  
350 small amounts of SO<sub>2</sub> may be present in emissions from Krýsuvík. Magmatic SO<sub>2</sub> might be able to ascend rapidly to the surface during  
351 periods of high seismicity. Another potential source of SO<sub>2</sub> is near surface oxidation of H<sub>2</sub>S to SO<sub>2</sub> (Arnórsson, 1987).

352 Eruptive activity of volcanic systems on RP is characterised by decades-long episodes of fissure eruptions. Based on eruption history,  
353 Krýsuvík may enter the next episode within the next decades. During eruptive activity, changes in fumarolic gas composition are likely to  
354 occur. Several studies (e.g., Noguchi and Kamiya 1963, Casadevall et al., 1983, Fischer and Arehart, 1996) have shown changes in the  
355 fumarole gas composition prior to and during eruptive events. Studies from the rifting episodes in Krafla, NE-Iceland during 1975-1984 (a

356 volcanic system which bears many similarities to Krýsuvík), revealed changes in local fumarolic gas composition (e.g., Óskarsson, 1984,  
357 1978, Gíslason et al., 1984). The gas composition was CO<sub>2</sub>-rich during the first weeks of rifting and remained unchanged until 1983. The  
358 outgassing CO<sub>2</sub> was released from the deep aquifers beneath the area by the interaction of magmatic gas with the hydrothermal system.  
359 A comprehensive record and monitoring in the Krýsuvík region would be a great asset in understanding of the gas source and the degassing  
360 regime of Krýsuvík. When new magma intrudes into the roots of the Krýsuvík system, the fumarolic gas composition can be expected to  
361 change similar to what was seen at Krafla 1975-1984 (e.g., Óskarsson, 1984, 1978, Gíslason et al., 1984). The gas composition in Krýsuvík  
362 would be expected to become CO<sub>2</sub> richer, resulting in lowering of H<sub>2</sub>O/CO<sub>2</sub>, and increase in CO<sub>2</sub>/H<sub>2</sub>S MultiGAS and fumarole ratios. The  
363 CO<sub>2</sub> gas fluxes are expected to increase as well.  
364 Several smaller localities with apparent surface activity (mostly related to the Trölladyngja subarea) were not measured as part of this study.  
365 We therefore conclude that the total soil CO<sub>2</sub> flux from the Krýsuvík geothermal system during this study is higher than 101 T/day.  
366 Furthermore, the total CO<sub>2</sub> soil flux estimated here should be considered as the minimum value given that the amount of CO<sub>2</sub> dissolved in  
367 groundwater is unknown.  
368 The total measured soil CO<sub>2</sub> flux from the neighbouring Reykjanes (~0.4 km<sup>2</sup>) and Hengill volcanic systems (168 km<sup>2</sup>) (using the  
369 accumulation chamber method) indicate total soil CO<sub>2</sub> flux of 78.5±13.9 T/day (Óladóttir, 2014) and 1,526 ± 160 T/day of which 453 T/day of  
370 volcanic/hydrothermal origin (Hernández et al., 2012), respectively. Studies of the volcanic systems along the RP during the last decades  
371 show little evidence of magmatic contribution with the exception of the Hengill volcano (Hreinsdóttir et al., 2001, Einarsson, 2008, Keiding et  
372 al., 2008), which suggested minor magma injection into the roots of the volcano from 1995 to 1998 that triggered an intense seismic swarm  
373 (Sigmundsson et al., 1997).  
374 It is important to continue the monitoring of gas emissions in Krýsuvík, at least over the next episode of land uplift and elevated seismicity to  
375 compare with the dataset from this study. It would be of particular interest to observe if changes in the gas composition will occur during  
376 inflation episode, as that will give important information on the source of the inflation.

## 377 **5 Conclusions**

378 The gas composition from the Krýsuvík geothermal system was studied (April-November 2013) using the MultiGAS method and correlated  
379 with geophysical observations. The gas composition is H<sub>2</sub>O dominated with CO<sub>2</sub> as the dominant dry gas species, with lesser amounts of H<sub>2</sub>S  
380 and trace amounts of SO<sub>2</sub>.

381 The gas emissions (in the form of diffuse soil degassing) were measured in three areas of high geothermal surface activity within the Krýsuvík  
382 system (Seltún, Hveradalir and Austurengjar). The total emission is estimated as 101 T/day but gives a minimum value for the total emission,  
383 as the amount of CO<sub>2</sub> dissolved in groundwater is not known and several smaller localities with apparent surface activity were not measured.

384 The time series of gas composition (MultiGAS data) identified short-lived episodes of elevated and highly variable H<sub>2</sub>O/CO<sub>2</sub> and H<sub>2</sub>O/H<sub>2</sub>S  
385 ratios (the highest H<sub>2</sub>O/CO<sub>2</sub> and H<sub>2</sub>O/H<sub>2</sub>S ratios followed periods of highest accumulative seismic moment per day (26 April 2013 and 11 July  
386 2013). SO<sub>2</sub> is detected at the same time. Correlation with seismicity and ground deformation shows that the ratio peaks follow increased  
387 seismic activity, with the highest H<sub>2</sub>O/CO<sub>2</sub> and H<sub>2</sub>O/H<sub>2</sub>S ratios following elevated seismicity and crustal movements. It is proposed that these  
388 peaks represent periods of elevated fumarolic activity that are responding to the seismicity and land uplift due to opening of new pathways in  
389 the crust and increased boiling within the system. During these periods the steam reaches the inlet tube faster and is less affected by pre-  
390 sampling H<sub>2</sub>O condensation. The CO<sub>2</sub> and H<sub>2</sub>S gases are significantly less affected by condensation processes and the CO<sub>2</sub>/H<sub>2</sub>S ratio does not  
391 change according to the same pattern. Most of the measured CO<sub>2</sub>/H<sub>2</sub>S ratios fall within the known range for Krýsuvík fumaroles. However,  
392 several markedly higher values are detected, demonstrating more variability in the degassing system than previously known.

393 It is considered crucial to continue the MultiGAS measurements in the Krýsuvík geothermal due to recent episodes of ground uplift and  
394 subsidence as well as future volcanic activity. During the span of the MultiGAS measurements in 2013 the total subsidence in the area was ~21  
395 mm.

## 396 **Acknowledgements**

397 Support for this work was received from the European Community's Seventh Framework Programme Grant No. 308377 (Project  
398 FUTUREVOLC), the Icelandic Research Fund No 110242011 (Project Volcano Anatomy) and No 100241021 (inflation of geothermal areas),  
399 and GEORG (Deep Roots of Geothermal systems). Seismic and meteorological data from the Icelandic Meteorological Office.

400

401 **References**

- 402 Adelinet, M., Dorbath, C., Ravalec, M, Le., Fortin, J., Guéguen, Y., 2011. Deriving microstructure and fluid state within the Icelandic crust  
403 from the inversion of tomography data. *Geophys. Res. Lett.* 38, L03305
- 404 Arnórsson, S., 1986. Chemistry of gases associated with geothermal activity and volcanism in Iceland: a review. *J. Geophys. Res* 91, 12261-  
405 12268.
- 406
- 407 Arnórsson, S., 1987. Gas chemistry of the Krísuvík geothermal field, Iceland, with special reference to evaluation of steam condensation in  
408 upflow zones. *Jökull* 37, 30-47.
- 409 Arnórsson, S., D'Amore, F., 2000. Geothermometry. In Arnórsson, S., *Isotopic and chemical techniques in geothermal exploration,*  
410 *development and use.* Vienna, International Atomic Energy Agency, 152-199.
- 411 Arnórsson, S., Gunnlaugsson, E., 1985. New gas geothermometers for geothermal exploration-Calibration and application. *Geochim.*  
412 *Cosmochim. Acta.* 49, 1307-1325.
- 413 Arnórsson, S., Fridriksson, Th., Gunnarsson, I., 1998. Gas chemistry of the Krafla geothermal field, Iceland. *Water-Rock interaction,* Arehart  
414 and Hulston, Balkema, Rotterdam.
- 415 Arnórsson, S., Guðmundsson, G, Sigurmundsson, S, G., Björnsson, A., Gunnlaugsson, E., Gíslason, G., Jónsson, J., Einarsson, P., Björnsson,  
416 S., 1975. Systematic exploration of the Krísuvík high-temperature area, Reykjanes-Peninsula, Iceland. Report, National Energy Authority,  
417 Reykjavik, Iceland. OS/JHD 7554, 127 pp.
- 418 Aiuppa, A., Burton, M., Caltabiano, T., Giudice, G., Guerrieri, S., Liuzzo, M., Muré, F., Salerno., G., 2010. Unusually large magmatic CO<sub>2</sub>  
419 gas emissions prior to a basaltic paroxysm. *Geophys. Res. Lett.* 37, 1-5.
- 420 Aiuppa, A., Federico, C., Giudice, G., Giuffrida, G., Guida, R., Guerrieri, S., Liuzzo, M., Moretti, R., Papale, P., 2009. The 2007 eruption of  
421 Stromboli volcano; Insights from real-time measurement of the gas volcanic plume CO<sub>2</sub>/SO<sub>2</sub> ratio. *J.Volc.Geoth. Res.* 182, 221-230.  
422
- 423 Ármannsson, H., Hauksson, H., 1980. Krafla, gas composition from fumaroles (in Icelandic). Report OS80027/JHD16, 48 pp.  
424

425 Ármannsson, H., Benjamínsson, J., Jeffrey, A. W. A., 1989. Gas changes in the Krafla geothermal system, Iceland. *Chem. Geol.* 76, 175-196.  
426  
427 Ármannsson, H., Gíslason, G., Hauksson, T., 1981. Magmatic gases in well fluids aid the mapping of the flow pattern in a geothermal system.  
428 *Geochim. Cosmochim. Acta.* 46, 167-177.  
429  
430 Brombach, T., Hunziker, J.C., Chiodini, G., Cardellini, C., Marini, L., 2001. Soil diffuse degassing and thermal energy fluxes from the  
431 southern Lakki plain, Nisyros (Greece). *Geophys Res. Lett.* 28, 69–72.  
432  
433 Cardellini, C., Chiodini, G., Frondini, F., 2003. Application of stochastic simulation to CO<sub>2</sub> flux from soil: Mapping and quantification of gas  
434 release. *J. Geophys. Res* 108, B9.  
435  
436 Casadevall, T. J., Rose, W., Gerlach, T., Greenland, L. P., Ewert, J., Wunderman, R., Symonds, R., 1983. Gas emissions and eruptions. Mount  
437 St. Helens through 1982. *Science* 221, 1383-1385.  
438  
439 Chiodini, G., Frondini, F., Cardellini, C., Granieri, D., Marini, L., Venura, G., 2001. CO<sub>2</sub> degassing and energy release at Solfatara volcano,  
440 Campi Flegrei, Italy. *J. Geophys. Res* 106, 16,213-16,221.  
441  
442 Chiodini, G., Cioni, R., Guidi, R., Raco, B., Marini, L., 1998. Soil CO<sub>2</sub> flux measurements in volcanic and geothermal areas. *Appl. Geochem.*  
443 13, 543-552  
444  
445 Clifton, A. E., Katterhorn, S. A., 2006. Structural architecture of a highly oblique divergent plate boundary segment. *Tectonophysics* 419, 27-  
446 40.  
447 .  
448 Didana, Y. L., 2010. Multidimensional Inversion of MT data from Krýsuík high temperature geothermal field, SW-Iceland, and a study of  
449 how 1D and 2D inversion can reproduce a given 2D/3D resistivity structure using synthetic MT data. Unpublished MS thesis, University of  
450 Iceland, Reykjavik, 119 pp.

451 Einarsson, P., 2008. Plate boundaries, rifts and transforms in Iceland. *Jökull* 58, 35-58.  
452  
453 Fischer, T. P., Arehart, G. B., 1996. The relationship between fumarole gas composition and eruptive activity at Galeras volcano. *Geology* 24,  
454 531.



455  
456 Fridriksson, Th., Kristjánsson, B. R., Ármannsson, H., Margrétardóttir, E., Ólafsdóttir, S., Chiodini, G., 2006. CO<sub>2</sub> emission and heat flow  
457 through soil, fumaroles, and steam heated mud pools at the Reykjanes geothermal area, SW-Iceland. *Appl. Geochem.* 21, 1551-1569.  
458  
459 Gíslason, G., Ármannsson, H., Hauksson, T., 1978. Krafla, Temperature conditions and gas species within the geothermal system (in  
460 Icelandic). Orkustofnun Report OSJHD-7846, 45 pp.  
461  
462 Gíslason, G., Johnsen, G. V., Ármannsson, H., Torfason, H., Árnason, K., 1984. Surface explorations in the Theistareykir high-temperature  
463 area (in Icelandic). Orkustofnun Report OS-84089/JHD-16, 138 pp.  
464  
465 Goff, F., Janik, C. J., 2000. Geothermal systems. In Sigurdsson, H (editor in chief), Houghton, B., McNutt, S. R., Rymer, H., Stix, J., 2000.  
466 *Encyclopedia of Volcanoes*. San Diego, California: Academic Press, 817-834.

467 Guðmundsson, G., Arnórsson, S., Sigurmundsson, S. G., Björnsson, A., Gunnlaugsson, E., Gíslason, G., Jónsson, J., Einarsson, P., Björnsson,  
468 S., 1975. The Krýsuvík area, report on geothermal observations (in Icelandic). Report OSJHD 7554, November 1975, 71 pp.  
469

470 Gutenberg, B., Richter, C.F., 1944. Frequency of earthquakes in California. *Bull. Seismol. Soc. Am.* 34, 185–188.

471 Hernández, P. A., Pérez, N. M., Fridriksson, Th., Egbert, J., Ilyinskaya, E., Thórhallsson, A., Ívarsson, G., Gíslason, G., Gunnarsson, I.,  
472 Jónsson, B., Padrón, E., Melián, G., Mori, T., Notsu, K., 2012. Diffuse volcanic degassing and thermal energy release from Hengill volcanic  
473 system, Iceland. *Bull Volcanol*, 74, 2435-2448.

474 Hanks, T. and Kanamori, H., 1979. A moment magnitude scale, *J. Geophys. Res.*, 84, No. B5, 2348-2350.

475 Hersir, G., Árnason, K., Vilhjálmsson, A., 2013. 3D inversion of Magnetotelluric (MT) resistivity data from Krýsuvík high temperature  
476 geothermal area in SW Iceland. *PROCEEDINGS, Thirty-eighth workshop on Geothermal Reservoir Engineering*, Stanford University,  
477 Stanford, California, February 11-13, 2013. SGP-TR-198. 14 pp.  
478  
479 Hreinsdóttir, S., Einarsson, P., Sigmundsson, F., 2001. Crustal deformation at the oblique spreading Reykjanes Peninsula, SW Iceland: GPS  
480 measurements from 1993 to 1998. *J. Geophys. Res.* 106, 13803-13816.  
481

482 Ilyinskaya, E., Aiuppa, A., Bergson, B., Di Napoli, R., Fridriksson, T., Oladottir, A. A., Oskarsson, F., Grassa, F., Pfeffer, M., Lechner, K.,  
483 Yeo, R., Giudice, G., 2014. Degassing regime of Hekla volcano 2012-2013. *Geochim. Cosmochim. Acta.* 159, 80-99.

484 Italiano, F., Pecoraino, G., Nuccio, P. M., 1998. Steam output from fumaroles of an active volcano: Tectonic and magmatic-hydrothermal  
485 controls of the degassing system at Vulcano (Aeolian Arc). *J. Geophys. Res.* 103, 29829-29842.

486

487 Jónsson, J., 1978. Geological map of the Reykjanes peninsula (In Icelandic). Orkustofnun Report OS JHD 7831, 347 pp. + maps.

488

489 Keiding, M., Árnadóttir, T., Sturkell, E., Geirsson, H., Lund, B., 2008. Strain accumulation along an oblique plate boundary: the Reykjanes  
490 Peninsula, southwest Iceland. *J. Geophys. Res.* 113, 861-872.

491 Keiding, M., Lund, B., Árnadóttir, T., 2009. Earthquakes, stress, and strain along an obliquely divergent plate boundary: Reykjanes Peninsula,  
492 southwest Iceland. *J. Geophys. Res.* 114, 1978-2012.

493

494 Klein, F. W., Einarsson, P., Wyss, M., 1977. The Reykjanes Peninsula, Iceland earthquake swarm of September 1972 and its tectonic  
495 significance. *J. Geophys. Res.* 82, 865-888.

496

497 Kristjánsdóttir, S., 2013. Microseismicity in Krýsuvík Geothermal Field, SW Iceland, from May to October 2009. Unpublished MS-thesis,  
498 University of Iceland, Reykjavik, 50 pp.

499

500 Lee, H. F., Yang, T. F., Lan, T. F., Song, S. R., Tsao, S., 2005. Fumarolic Gas Composition of the Tatun Volcano Group, Northern Taiwan.  
501 *TAO* 16, 843-864.

502

503 Markússon, S., Stefánsson, A., 2011. Geothermal surface alteration of basalts, Krýsuvík Iceland-Alteration mineralogy, water chemistry and  
504 the effects of acid supply on the alteration process. *J. Volc. Geoth. Res.* 206, 46-59.

505

506 Michalczewska, K., Hreinsdóttir, S., Arnadóttir, T., Hjaltadóttir, S., Agustsdóttir, T., Gudmundsson, M.T., Geirsson, H., Sigmundsson, F.,  
507 Gudmundsson, G., 2012. Inflation and deflation episodes in the Krisuvik volcanic system, Abstract V33A-2843, *Am. Geophys. Un.* Fall  
508 meeting, San Francisco, December 2012. Available on: <http://fallmeeting.agu.org/2012/eposters/eposter/v33a-2843/>. 1 pp.

509

510 Noguchi, K., Kamiya, H., 1963. Prediction of volcanic eruption by measuring the chemical composition and amounts of gases. *Bull. Volcanol.*  
511 26, 367-378.

- 512  
513 Óladóttir, A. A., 2012. Application of soil measurements and remote sensing for monitoring changes in geothermal surface activity in the  
514 Reykjanes field, Iceland. Unpublished MS thesis, University of Iceland, Reykjavik, 110 pp.  
515
- 516 Óladóttir, A. A., 2014. The observations on CO<sub>2</sub> flux through soil and soil temperature in the Reykjanes geothermal area in 2012 and 2013.  
517 Report, ÍSOR-2014/024. 27 pp.  
518
- 519 Óskarsson, N., 1984. Monitoring of fumarole discharge during the 1975-1982 rifting in Krafla volcanic center, north Iceland. J. Volc. Geoth.  
520 Res. 22, 97-121.  
521
- 522 Óskarsson, N. 1978. Effect of magmatic activity on fumarole gas composition in the Námafjall-Krafla volcanic center, N-Iceland. NVI  
523 Research Report 7803.  
524
- 525 Saemundsson, K., Jóhannesson, H., 2006. On the likelihood of lava flows and ash fall between hafnasfjörður and keflavík (In Icelandic).  
526 Report, ÍSOR-2006/001, 26 pp.
- 527 Saemundsson, K., Jóhannesson, H., Hjartarson, Á., Kristinsson, S, G., Sigurgeirsson, M, Á., 2010. Geological Map of Southwest Iceland.  
528 1:100000. Reykjavík: Iceland GeoSurvey.
- 529 Saemundsson, K., Sigurgeirsson, M, Á., 2013. The Reykjanes Peninsula. In Sólnes, J (editor in chief), Sigmundsson, F., Bessason, B., 2013.  
530 Natural hazards in Iceland, volcanic eruptions and earthquakes (in Icelandic). Reykjavík, Viðlagatrygging Íslands/Háskólaútgáfan, 379-403.
- 531 Schorlemmer, D., Weimer, S., Wyss, M., 2005. Variations in earthquake size distribution across different stress regimies. Nature 437, 539-  
532 542.
- 533 Sigmundsson, F., Einarsson, P., Rögnvaldsson, Th., Foulger, G., Hodkinson, Kþ. Thorbergsson, G., 1997. The 1994-1995 seismicity and  
534 deformation at the Hengill triple junction, Iceland: Triggering of earthquakes by an inflating magma chamber in a zone of horizontal shear  
535 stress. J. Geophys. Res. 102, 15151-15161.
- 536 Toutain, J, P., Baubron, J, C., 1999. Gas geochemistry and seismotectonics: a review. Tectonophysics 304, 1-27.  
537
- 538 Ward, P. L., Björnsson, S., 1971. Microearthquakes, swarms, and the geothermal areas of Iceland. J. Geophys. Res. 76, 3953-3982.

539

540 Watson, I. M., Oppenheimer, C., Voight, B., Francis, P. W., Clarke, A., Stix, J., Miller, A., Pyle, D. M., Burton, M. R., Young, S. R., Norton,  
541 G., Loughlin, S., Darroux, B., MVO staff., 2000. The relationship between degassing and ground deformation at Soufriere Hills Volcano,  
542 Montserrat. *J. Volc. Geoth. Res.* 98, 117-126.

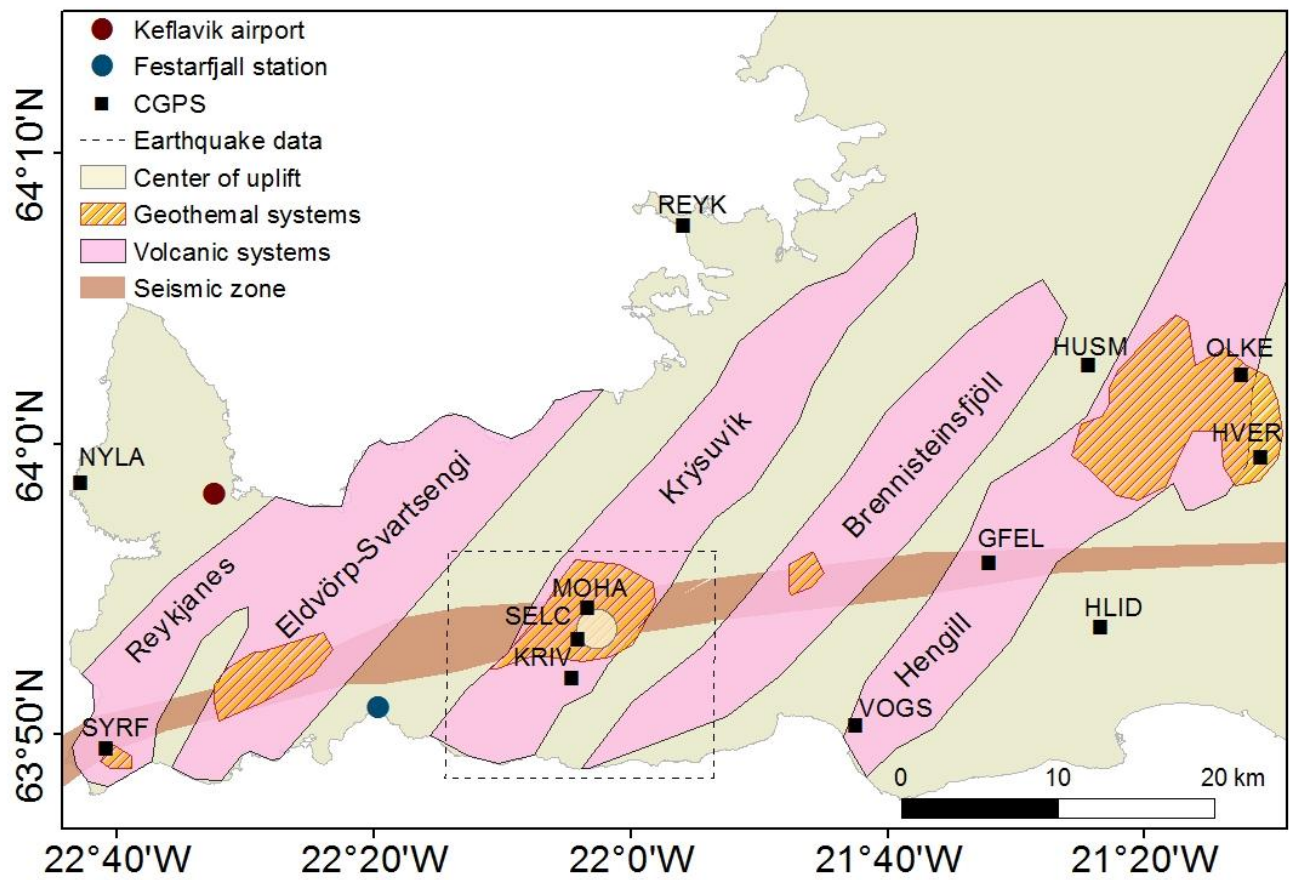
543 Wyss, M., 1973. Towards a physical understanding of the earthquake frequency distribution, *Geophys. J. Int.*, 31, 341–359.

544 Yohannes B., E., 2004. Geochemical interpretation of thermal water and gas samples from Krýsuvík, Iceland and Alid, Eritrea. In L.S.  
545 Georgsson, Editor. *Geothermal Training in Iceland 2004*. UNU Geothermal Training Programme Report 18, 403-438.

546 Young, S. R., Francis, P. W., Barclay, J., Casadeva, T. J., Gardner, C. A., Darroux, B., Davies, M. A., Delmelle, P., Norton, G. E.,  
547 Maciejewski, A. J. H., Oppenheimer, C. M. M., Stix, J., Watson, I. M., 1998. Monitoring SO<sub>2</sub> emission at the Soufriere Hills volcano:  
548 Implications for changes in eruptive conditions. *Geophys. Res. Lett.* 25, 3681-3684.

549

550



551

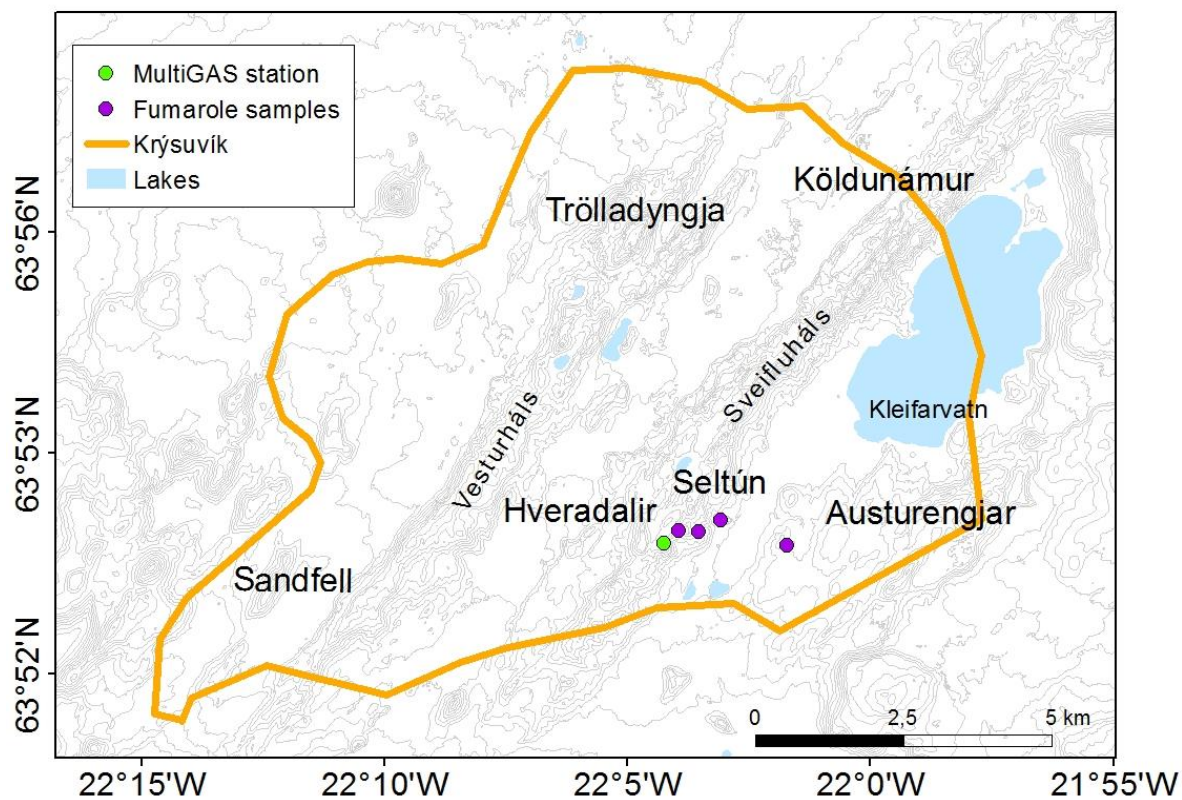
552

553 **Figure 1** Volcanic systems on the RP (purple) and seismic zone across the Peninsula that marks the axis of the plate boundary (brown) (Einarsson, 2008). High-  
 554 temperature geothermal areas within the volcanic systems (striped). Modified from (Sæmundsson and Sigurgeirsson, 2013). The five volcanic systems are arranged en  
 555 echelon along the peninsula, spaced approximately 5 km apart (Clifton et al., 2006). Continuous GPS stations in operation in 2013 on the RP including the region of the

556 earthquake data (dashed box), and the center of uplift (yellow circle). Blue and dark red dots show the location of Festafjall and Keflavík airport weather stations,  
557 respectively.

558

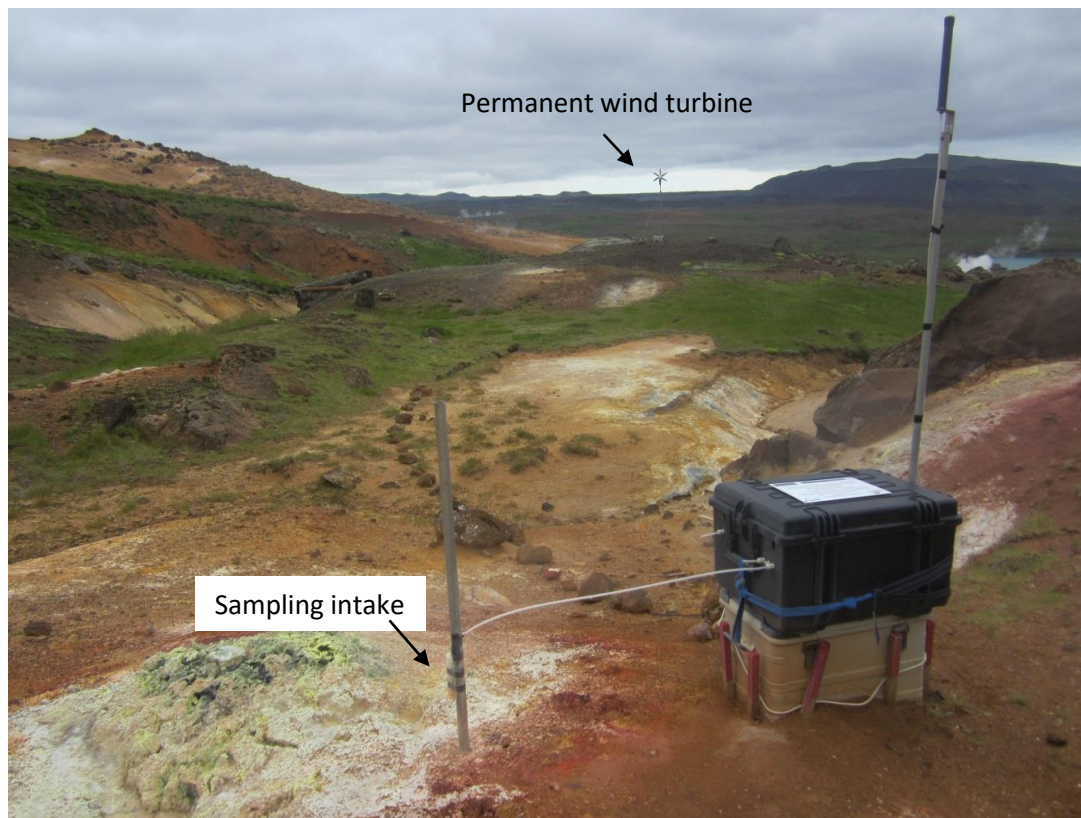
559



560

561 **Figure 2** Outlines of the Krýsuvík high-temperature geothermal system identified by resistivity surveys (orange line) (Gudmundson et al., 1975). Krýsuvík sub-areas and  
562 the two hyaloclastite ridges, Sveifluháls and Vesturháls, with which the geothermal activity in Krýsuvík is mostly associated.

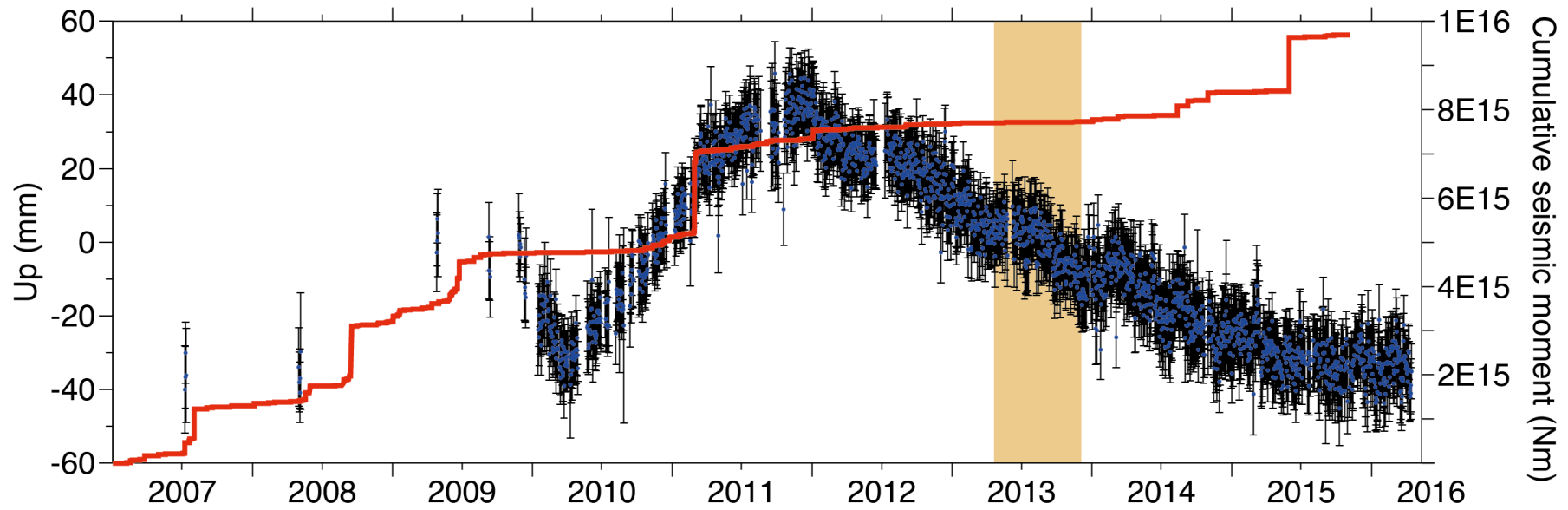




563

564 **Figure 3** MultiGAS station in Krýsuvík. The station is located next to a fumarole in an area of continuous geothermal activity in Hveradalir, Krýsuvík, and is powered by  
565 a wind turbine. The sampling inlet of the MultiGAS station is located ~20 cm above the ground to avoid saturation of the CO<sub>2</sub> sensor.

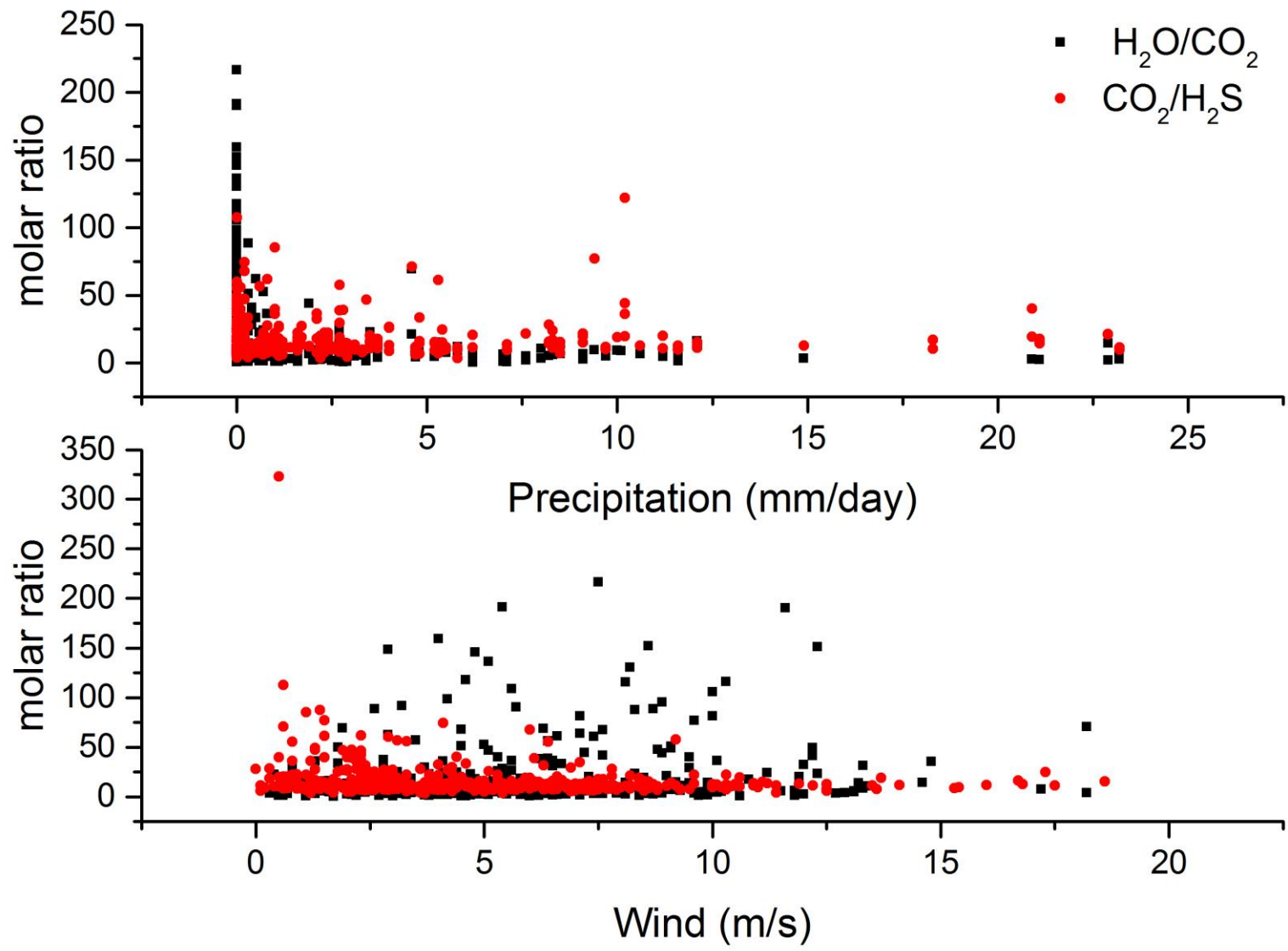




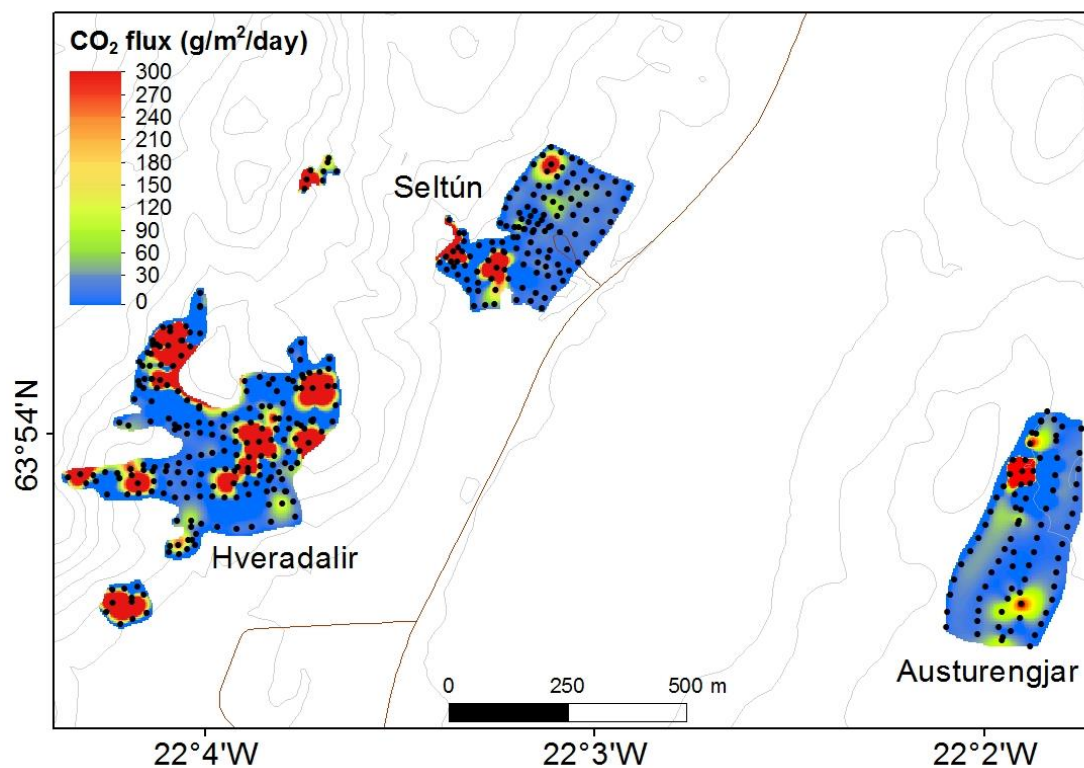
566

567  
568

**Figure 4** The local inflation/deflation periods from GPS time series (2007-2016) at station MOHA, along with daily cumulative seismic moment. The red band corresponds to the time period of this study.



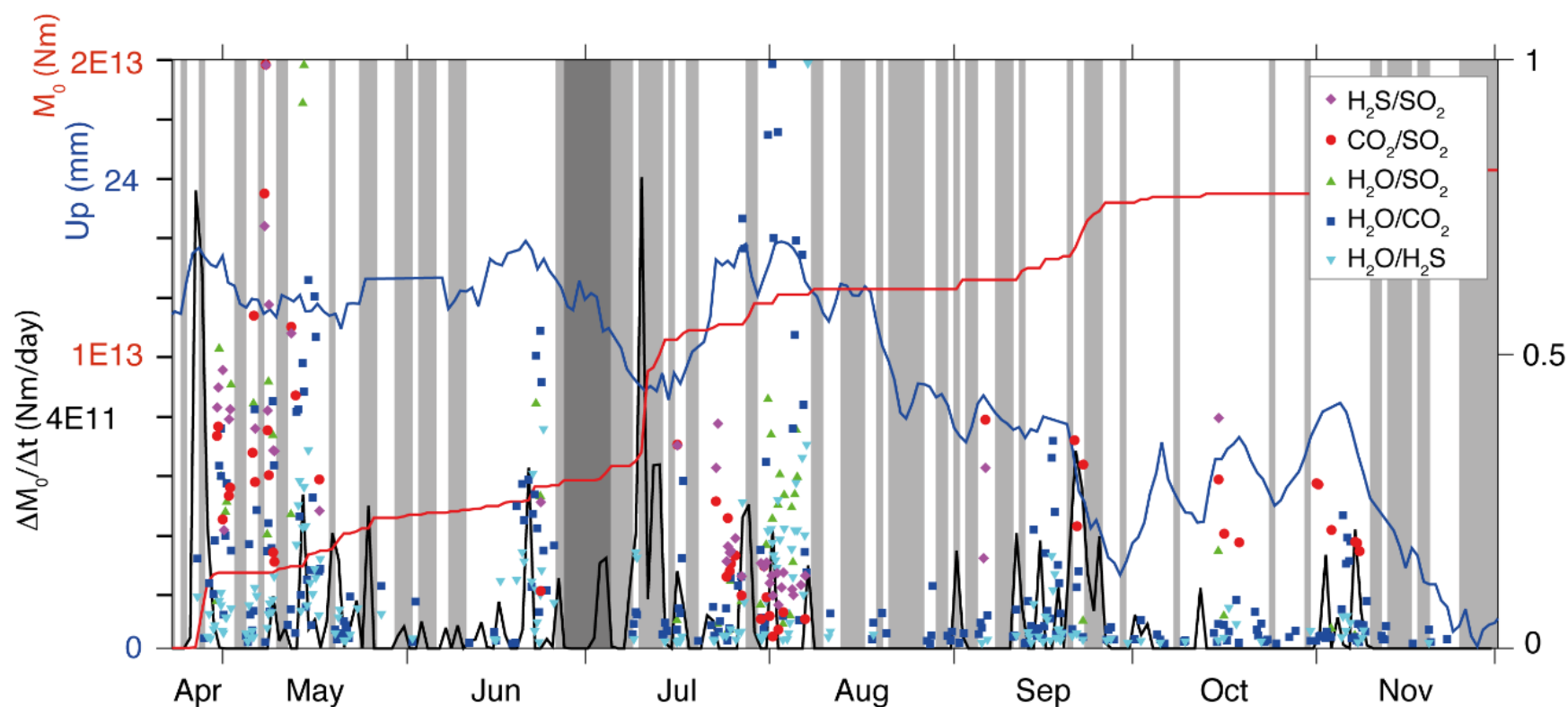
570 **Figure 5** (Upper)  $\text{CO}_2/\text{H}_2\text{S}$  and  $\text{H}_2\text{O}/\text{CO}_2$  molar ratios as a function of precipitation (mm/day). The  $\text{CO}_2/\text{H}_2\text{S}$  ratio are obtained predominantly during periods with <2  
571 mm/day rainfall. However, high ratio values are not confined to the dry periods. All  $\text{H}_2\text{O}/\text{CO}_2$  ratios >19 are obtained during dry periods (< 2mm/day). The most  
572 frequently obtained values for  $\text{H}_2\text{O}/\text{CO}_2$  (<19) are visually evenly distributed between ~ 0-5 mm/day. (Lower)  $\text{CO}_2/\text{H}_2\text{S}$  and  
573  $\text{H}_2\text{O}/\text{CO}_2$  molar ratio as a function of wind speed (m/s). The highest ratios of  $\text{CO}_2/\text{H}_2\text{S}$  (>75) and largest variations are obtained during relatively low wind speed  
574 (approximately <5 m/s). Lower values of  $\text{CO}_2/\text{H}_2\text{S}$  (<20) are detected more frequently than the higher values and there is no visible relation to wind speed <10 m/s where  
575 marked decrease is seen in the frequency of ratios obtained. Wind speed <10 m/s does not appear to affect detection of  $\text{H}_2\text{O}/\text{X}$  molar ratios (X =  $\text{CO}_2$ ,  $\text{H}_2\text{S}$  and  $\text{SO}_2$ ) in >10  
576 m/s markedly fewer ratios are detected.



577

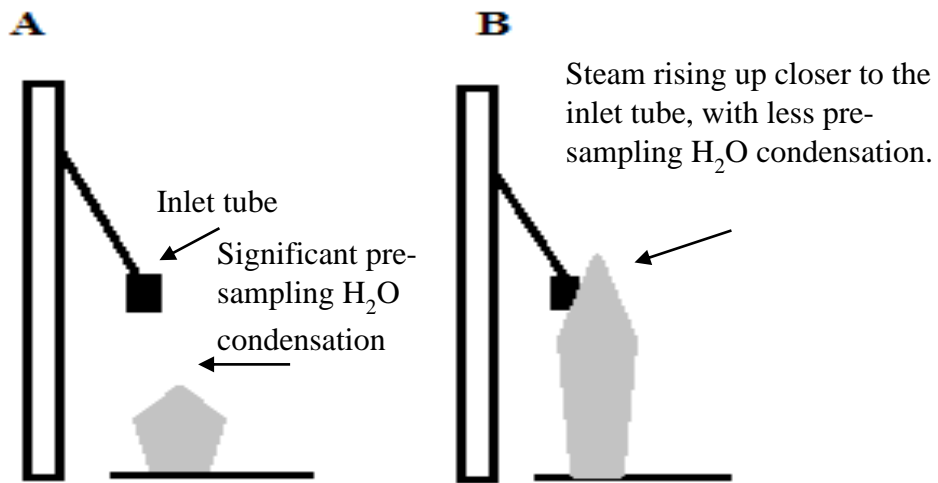
578 **Figure 6** Soil CO<sub>2</sub> flux measurements from the three observation areas, Hveradalir, Seltún, and Austurengjar. The highest flux was observed in Hveradalir, 70.9 T/day. In  
 579 Seltún the flux was found to be 19.6 T/day and the lowest flux was calculated in Austurengjar, 10.9 T/day. The total flux from the three measured areas was calculated as  
 580 101 T/day.

581



582

583 **Figure 7** Normalized variations in gas composition as measured by the MultiGAS station (measurements affected by metrological conditions have been eliminated)  
 584 correlated with geophysical observations. There are distinct intervals with peaks of increased H<sub>2</sub>O/CO<sub>2</sub> and H<sub>2</sub>O/H<sub>2</sub>S ratios. SO<sub>2</sub> is detected during the same intervals  
 585 allowing calculation of X/SO<sub>2</sub> ratios. Red line: cumulative seismic moment (Nm). Black line: seismic moment per day (Nm/day). Blue curve: Vertical crustal movements  
 586 measured with GPS (mm). Light grey intervals: rainy days (>2 mm/day). Dark grey interval: station not operating. Peaks of increased H<sub>2</sub>O/CO<sub>2</sub> and H<sub>2</sub>O/H<sub>2</sub>S ratios appear  
 587 to follow episodes of recorded seismic events and crustal deformation.



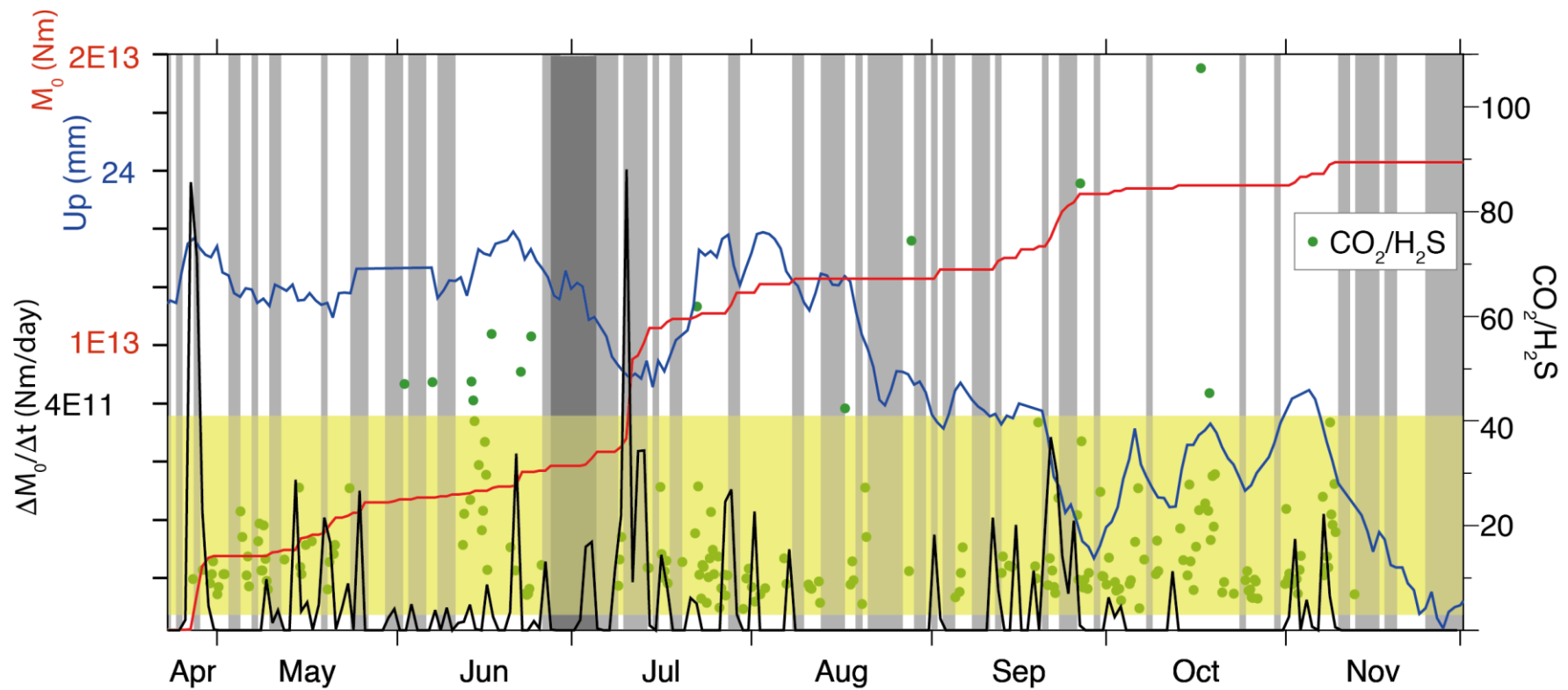
588

589 **Figure 8** A) Lower fumarole activity resulting in low H<sub>2</sub>O/CO<sub>2</sub> and H<sub>2</sub>O/H<sub>2</sub>S gas ratios measured by MultiGAS. The cause is condensation of H<sub>2</sub>O before the gas reaches  
 590 the inlet tube (20 cm above the ground). These low ratios are not representative of the fumarolic gas composition. B) Higher fumarole activity due to crustal movements.  
 591 The steam is less affected by pre-sampling condensation resulting in higher H<sub>2</sub>O/CO<sub>2</sub> and H<sub>2</sub>O/H<sub>2</sub>S ratios. These values are closer to the H<sub>2</sub>O/CO<sub>2</sub> and H<sub>2</sub>O/H<sub>2</sub>S ratios as  
 592 measured in direct samples of the fumaroles.

593

594

595



596

597 **Figure 9** Time series (April-November 2013) of CO<sub>2</sub>/H<sub>2</sub>S MultiGAS molar ratios (where measurements effected by metrological conditions have been eliminated)  
 598 compared with crustal movements. The CO<sub>2</sub>/H<sub>2</sub>S ratio does not show any visible variations related to seismicity or crustal deformation. The yellow band corresponds to  
 599 CO<sub>2</sub>/H<sub>2</sub>S ratios (3-41) from fumaroles in the Krýsuvík area (this study, Arnórsson, 1987, data from the Iceland GeoSurvey database).

600

601

602

603

604

605

606

607

608

609

610

611

612

613

614

615

616

617

618

619

620

621



622

623

624

625

626 **Table 1** *Vol% concentration in fumarolic steam from the 8 samples. Values within ( ) for CO<sub>2</sub> and H<sub>2</sub>S refer to % of total gas volume.*

<b>Sample</b>	<b>Date</b>	<b>H<sub>2</sub>O%</b>	<b>CO<sub>2</sub>%</b>	<b>H<sub>2</sub>S%</b>	<b>H<sub>2</sub>%</b>	<b>Ar%</b>	<b>O<sub>2</sub>%</b>	<b>N<sub>2</sub>%</b>	<b>CH<sub>4</sub>%</b>
<b>Seltún 1</b>	18.02.2014	96.9	75.5 (2.3)	13.9 (0.430)	9.32	0.02	0.15	1.03	0.08
<b>Seltún 2</b>	23.04.2014	99.4	79.6 (0.48)	15.3 (0.092)	4.80	-	-	0.32	0.02
<b>Hverahvammur 1</b>	18.02.2014	99.5	88.9 (0.44)	8.69 (0.043)	2.02	-	-	0.40	-
<b>Hverahvammur 2</b>	23.04.2014	99.4	89.3 (0.54)	9.26 (0.056)	0.97	-	-	0.49	-
<b>Austurengjar 1</b>	18.02.2014	99.4	89.3 (0.54)	3.80 (0.023)	6.13	-	-	0.67	0.10
<b>Austurengjar 2</b>	23.04.2014	99.5	81.5 (0.41)	12.9 (0.065)	5.36	-	-	0.19	0.06
<b>Hverahöfði 1</b>	18.02.2014	99.4	73.4 (0.44)	4.00 (0.024)	19.7	0.04	-	2.65	0.22
<b>Hverahöfði 2</b>	23.04.2014	99.6	93.2 (0.37)	5.54 (0.022)	0.76	-	-	0.49	0.02

627

628 **Table 2** *Variations of the molar gas ratios measured by the MultiGAS station in Hveradalir, Krýsuvík (excluding data affected by meteorological factors).*

	<b>Max</b>	<b>Min</b>	<b>Average</b>	<b>Median</b>
<b>H<sub>2</sub>O/CO<sub>2</sub></b>	217	1	27	9

<b>H<sub>2</sub>O/H<sub>2</sub>S</b>	10300	9	640	218
<b>H<sub>2</sub>O/SO<sub>2</sub></b>	107000	2380	26900	25100
<b>CO<sub>2</sub>/H<sub>2</sub>S</b>	107	4	17	12
<b>CO<sub>2</sub>/SO<sub>2</sub></b>	3010	58	767	662
<b>H<sub>2</sub>S/SO<sub>2</sub></b>	148	11	42	35

629

630 **Table 3** The calculated molar ratios of H<sub>2</sub>O/CO<sub>2</sub>, H<sub>2</sub>O/H<sub>2</sub>S and CO<sub>2</sub>/H<sub>2</sub>S for the fumarole samples and from the MultiGAS data. Sample Seltún 1 is excluded from the  
631 average calculations due to condensation in the sampling train. The maximum H<sub>2</sub>O/H<sub>2</sub>S values in the MultiGAS data (10300) is by far the highest value, the second  
632 highest value (3850) is, much closer to the average value of the fumarole samples.

	MultiGAS				Fumaroles								
Ratio	Max	Min	Average	Median	Seltún 2	Hvera- hvammur 1	Hvera- hvammur 2	Austur- engjar 1	Austur- engjar 2	Hvera- höfði 1	Hvera- höfði 2	Average	Median
<b>H<sub>2</sub>O/CO<sub>2</sub></b>	217	1	27	9.0	207	226	184	184	243	226	269	220	226
<b>H<sub>2</sub>O/H<sub>2</sub>S</b>	10300 (3850)	9	640	218	1080	2313	1775	4321	1530	4141	4527	2812	2313
<b>CO<sub>2</sub>/H<sub>2</sub>S</b>	107	4	17	12	5	10	10	24	6	18	17	13	10

634

635 **Table 4** Gas geothermometers applied to Krýsuvík fumarole samples.

Geothermometer	Temperature function <sup>1</sup>	Reference
CO <sub>2</sub>	$4.724Q^3 - 11.068Q^2 + 72.012Q + 121.8$	(Arnórsson et.al 1998)
H <sub>2</sub> S	$4.811Q^2 + 66.152Q + 177.6$	(Arnórsson et.al 1998)
H <sub>2</sub>	$6.630Q^3 + 5.836Q^2 + 56.168Q + 227.1$	(Arnórsson et.al 1998)
CO <sub>2</sub>	$-44.1 + 269.25Q - 76.88Q^2 + 9.52Q^3$	(Arnórsson and Gunnlaugsson 1985)
H <sub>2</sub> S	$173.2 + 65.04Q$	(Arnórsson and Gunnlaugsson 1985)
H <sub>2</sub>	$212.2 + 65.04Q$	(Arnórsson and Gunnlaugsson 1985)

636 <sup>1</sup>*Q* refers to the logarithm of the respective gas concentration or ratio in moles per kg of steam.637 **Table 5** The results from the applied gas geothermometers. The temperature value are in °C.

Sample	nr.	<sup>1</sup> CO <sub>2</sub>	<sup>1</sup> H <sub>2</sub> S	<sup>1</sup> H <sub>2</sub>	<sup>2</sup> CO <sub>2</sub>	<sup>2</sup> H <sub>2</sub> S	<sup>2</sup> H <sub>2</sub>	Average
Hverahvammur 1	1	292	276	274	288	261	259	275
Hverahvammur 2	2	303	268	256	295	270	243	272
Austurengi 1	3	301	255	323	294	244	295	285
Austurengi 2	4	289	290	309	286	273	286	289
Hverahöfði 1	5	292	257	281	288	245	266	271
Hverahöfði 2	6	292	259	244	288	247	231	260
Seltún 2	7	297	304	313	291	284	289	296

638